Skin pigmentation in snakes: a pattern formation approach

Javier Chico Vazquez[1]

Abstract A pattern formation approach is presented for the problem of snake skin pigmentation. Solutions showcasing stripes, spots, reticulated grids and plumes are found via numerical integration using spectral methods. Examples of irregular geometry breaking a pattern's symmetry are given.

1 Introduction

In Mathematical Biology, it is well established that in some dynamical systems, diffusion can lead to instability, instead of acting as smoothing operator, as it was believed for centuries. This instability phenomenon is named after its discoverer: *Turing instability* [1]. These instabilities often lead to pattern formation [2]. In the case of animals, when the quantities of interest are the concentration of chemical species (pigments) and their spatiotemporal evolution, this can lead to spots, stripes and other interesting fur patterns [3]. A common example of this are leopards, zebras etc...

The present paper will focus in extending this phenomena to growing domains. Most of the aforementioned models assume the domain is static in time [2]. However, this is not reasonable in numerous biological context, where the pattern development time scale is comparable with the embryonic growth time scale [4, 5], hence the domain growth must be accounted for. An application for this could be skin pigmentation in reptiles, fish or other animals with shorter incubation times or life spans or whose physiology allows them to continue growing even during adulthood. Particular emphasis will be placed in snakes, for they have relatively simple body shapes which allow for easier modeling, analysis and computation.

A chemotaxis based model as discussed by Murray et. al. [6] will be introduced to study pattern development in snakes, and criteria for pattern development will be studied. As motivation and preview, two snakes species with striking patterns are presented in Figure 1[2].

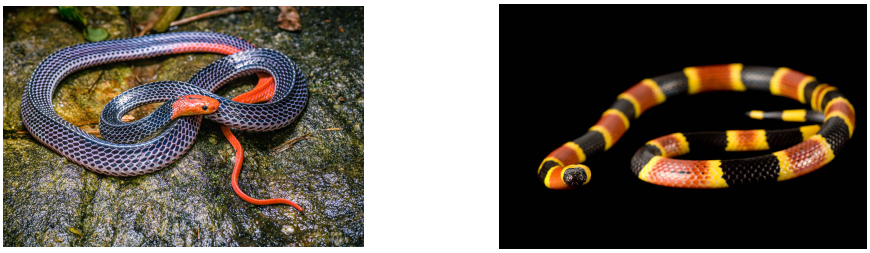

(a) *Bungarus flaviceps* (b) *Micrurus tener*

Figure 1: Some examples of striking snake patterns

This paper is organised in the following sections. In Section 2, the chemotaxis model is motivated, explained and formalised mathematically. Second, a first approach to pattern formation is introduced via linearization and the linear dispersion relation of the system is presented in Section 3, followed by a discussion of possible extensions. Finally, the patterns observed are presented alongside a discussion of their convergence and/or temporal behaviour, and the similarities and differences when compared to the results presented by Murray [6], followed by a brief conclusion. A brief discussion of the different computational techniques used to integrate the partial differential equations numerically is available in the appendix.

[1]Massachusetts Institute of Technology / Imperial College London

[2]Images from `https://www.thainationalparks.com/species/bungarus-flaviceps` and `https://www.nationalgeographic.org/projects/photo-ark/`

2 Description of the model

In this paper we focus on the nondimensional Cell-Chemotaxis model explored by Murray [6, 7, 8]

$$\partial_t n = D\nabla^2 n - \alpha\nabla\cdot(n\nabla c) + srn(N-n)$$

$$\partial_t c = \nabla^2 c + s\left[\frac{n}{1+n} - c\right]$$

where n and c denote the cell and chemoattractant densities. It is important to go over each of the individual terms to see what they represent. On the left hand side we have temporal derivatives which dictate that the system will evolve in time as prescribed by the right hand side. On the right hand side we have a Laplacian (∇^2 term for each chemical, which represents diffusion. In this case, as in many other pattern formation problems, it is important that the chemicals diffuse at different rates, as first described by Turing [1]). The next interesting term is the chemotaxis term, $\nabla\cdot(n\nabla c)$, which represents "the movement of cells in response to chemical gradients", as described by Hillen et. al. [9]. Finally, for the cell density equation we have a nonlinear term which models cell mitosis, $n(N-n)$. This logistic term will convey exponential growth when the cell density is small and it will limit growth when n is close to N. This term is responsible for the growth [7]. Finally, we have the nonlinear interaction terms for the chemoattractant, which are of the form, $\frac{n}{1+n} - c$. This models chemoattractant production. For more details please refer to [7].

Whilst Murray et. al. are interested in the steady state solutions [8], (namely setting the left hand side time derivatives equal to zero and solving the elliptic like equations that arise), this paper will focus in patterns which are dynamic both in space and time. We will work in a two dimensional rectangular domain. Unlike Murray et. al. which used Neumann/zero flux boundary conditions in every boundary, we will work with Neumann boundary conditions along the longitudinal/long axis of the snake, denoted as the y axis (visually, Neumann on the head and tail of the snake). However, in the interest of reproducing the snakes cylindrical geometry more faithfully, we will impose periodic boundary conditions along the horizontal axis of the snake, much like if the domain was a cylinder whose surface had been flattened. Hence mathematically,

$$\left.\frac{\partial n}{\partial y}\right|_{y=0, y=L_y} = 0 \quad \forall x \quad n(0,y) = n(L_x, y) \quad \forall y$$

The first step to analyze the equations is to look for homogeneous steady state solutions, i.e. solutions to

$$n(N-n) = 0 \quad \frac{n}{1+n} - c = 0$$

Apart from the trivial zero solutions we can see the solution $n_0 = N$, $c_0 = \frac{N}{1+N}$ is a homogeneous steady state. In the next section we will consider linear perturbation to this steady state.

3 Linearity analysis

We linearize around the homogenous steady state found in the previous section by defining

$$n = N + \epsilon u \quad \text{and} \quad c = \frac{N}{1+N} + \epsilon v$$

then we substitute, and keeping only terms of order $\mathcal{O}(\epsilon)$ we get the linear equations for u, v:

$$\partial_t u = D\nabla^2 u - \alpha N\nabla^2 v - srNu \quad \partial_t v = \nabla^2 v + s\left(\frac{u}{(1+N)^2} - v\right)$$

with the aforementioned boundary conditions on the boundary. We can find the dispersion relation by trying the following Ansatz and finding the characteristic polynomial of the matrix M

$$\begin{pmatrix} u \\ v \end{pmatrix} = \begin{pmatrix} \xi \\ \eta \end{pmatrix} e^{i\mathbf{k}\cdot\mathbf{x}+\sigma t} \quad \Longrightarrow \quad \sigma \begin{pmatrix} \xi \\ \eta \end{pmatrix} = \begin{pmatrix} -(Dk^2 + srN) & -k^2\alpha N \\ -s/(N+1)^2 & -(k^2+s) \end{pmatrix} \begin{pmatrix} \xi \\ \eta \end{pmatrix} := M \begin{pmatrix} \xi \\ \eta \end{pmatrix}$$

and the characteristic polynomial of M will be the implicit dispersion relation

$$\sigma^2 + [(D+1)k^2 + rsN + s]\sigma + \left[Dk^4 + \left(rsN + Ds - \frac{sN\alpha}{(1+N)^2}\right)k^2 + rNs^2\right] = 0$$

From the matrix we can also extract relevant information, such as the fastest growing mode, which will be the growth rate that will be observed experimentally.

$$\sigma_{max} = \frac{\partial_k \det(M)}{\partial_k \mathrm{Tr}(M)} = \frac{-2DN^2k^2 - DN^2s - 4DNk^2 - 2DNs - 2Dk^2 - Ds - N^2rs - 2Nrs + \alpha rs^2 - rs}{(D+1)\left(N^2+2N+1\right)}$$

If the node is stable then the snake will be monochromatic in terms of its skin patterns. To find unstable nodes, Murray [6] details a procedure to isolate a particular node that forces the pattern to grow initially. In particular, the isolated note satisfies $\sigma(k) = 0$, which combined with a uniqueness constraint on k means that the parameters satisfy

$$\left[srN + Ds - \frac{sN\alpha}{(1+N)^2}\right]^2 - 4Ds^2rN = 0$$

and under this constraint the critical wavevector $\mathbf{k_c}$ will have modulus $k_c^2 = \left[\frac{s^2rN}{D}\right]^2$. Now, following the procedure detailed in [8] we can use the above formulas to determine points in the parameter space were the critical wavevector is isolated. From here on, we will assume $N = s = 1$ and $D = 0.25$, and only treat α and r as *control* parameters, to replicate Murray's steps [7]. As for the length scales, $L_x = 1$ will be fixed and L_y will be varied to test the role of snake length in skin patterns.

4 Cylindrical domain and geometrical considerations

If we assume the chemicals are only in the surface then the problem is not much different. As $r = R$ is constant, we have $n = n(\theta, z, t)$ only (and same for c), so the differential operators are:

$$\nabla^2 = \frac{1}{R^2}\partial_{\theta\theta} + \partial_{zz} \quad \text{and} \quad \nabla \cdot (n\nabla c) = \frac{1}{R^2}\partial_\theta(n\partial_\theta c) + \partial_z(n\partial_z c)$$

and we would need to impose periodic boundary conditions on θ so that $n(0, z, t) = n(\pi, z, t)$ and $c(0, z, t) = c(\pi, z, t)$. This option is further explored in section 7.1.2. However, it is clear from the equations that they will be equivalent to the rectangular problem, as they only differ by a constant scale factor R^{-2}, and this effect can be reproduced by modifying the domain size L_x and L_y appropriately in the rectangular domain.

4.1 Full three dimensional cylindrical domain

A possible interesting extension is to consider solving the equations in the entire cylinder with $0 < r \leq R$, or between two coaxial cylinders, $R_0 < r \leq R$, modelling a skin layer. They could prove useful as the there are certain characteristics, such as a snake's curvature and its curled position during incubation which the two dimensional models can not incorporate. However, as it is not reasonable to expect a symmetry in the system which might allow us to remove one of the degrees of freedom and they are prohibitively expensive to solve with the author's available hardware it is not reasonable to solve them numerically.

Following this idea, it is also natural to consider non cylindrical domains. In fact many snakes are not cylindrical, some have triangular cross sections (*Bungarus fasciatus* and *Lachesis muta* are perhaps the most extreme examples), or have a boxy almost rectangular cross section (*Eunectes murinus*, and other Boas and Pythons), or a flattened tail enhanced for swimming as seen on sea snakes, e.g. *Laticauda*.

5 Results

The main result from the numerical simulations is that some patterns vary with time even after a long time, contrasting what Murray et. al. found with the bifurcating branch approach. All of the patterns presented by Murray [6] were replicated successfully with the exception of the longitudinal stripe. The exceedingly high value of $\alpha \sim 2000$ required proved to be problematic for the numerical procedures, that returned negative solutions. It was found that most unstable configurations lead to horizontal stripes, as suggested by Murray. However, there is a great diversity of different horizontal stripes, as seen in Figure [2], where the length of the snake is also varied. Moreover, some of these patterns are dynamic in time.

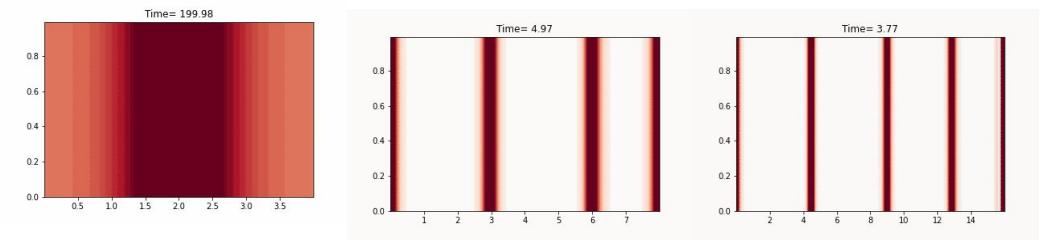

(a) Thick horizontal stripes ($\alpha = 12.31$, $r = 1.52$, as seen in *Bungarus fasciatus*

(b) Relatively thin horizontal stripes ($\alpha = 27.06$, $r = 1.52$)

(c) Very thin horizontal stripes ($\alpha = 29.61$, $r = 1.52$)

Figure 2: Horizontal stripe patterns

Other interesting patterns were observed when the parameter values were increased, suggesting the existence of a bifurcation at some point in the parameter space. Of particular interest are the reticulated patterns, as they are similar to those seen in the Reticulated Python. They are displayed in Figure 3 alongside a surprising steady pattern, a longitudinal plume like figure not discussed in previous literature, placed on one of the ends of the snake which could model species where pigmentation is accumulated on the extremities of the individual. Examples of this are *Bungarus flaviceps*, a snake member of the Krait family, displayed in Figure 1, or even Siamese cats, whose fur is mostly white except for a black a nose, tail and legs.

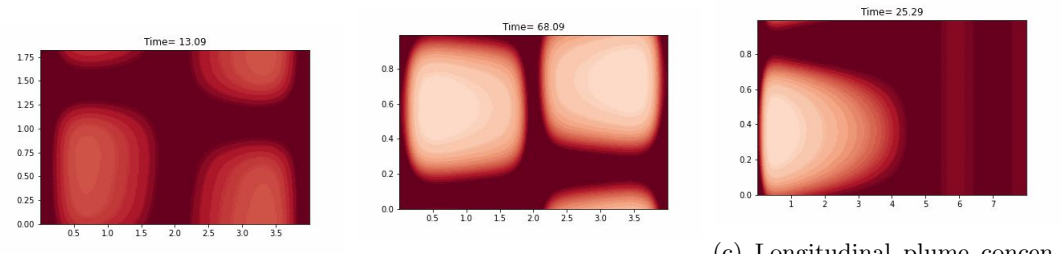

(a) Thick horizontal stripes ($\alpha = 177.7$, $r = 38.05$

(b) Quasi squares ($\alpha = 135.16$, $r = 28.22$), as seen in asian pythons

(c) Longitudinal plume concentrated on one of the snake's ends ($\alpha = 135.16$, $r = 28.05$), as seen in *Bungarus flaviceps*

Figure 3: Exotic patterns

Returning to the topic of longitudinal stripes, this is an area of open research, with Murakami et. al. [4] discussing the problem recently in great detail for the Japanese four-lined snake, without a mathematical model and a more experimentally focused approach.

5.1 Time dependent dynamic patterns

An unexpected result is that some of the patterns were dynamic in time. Whilst some showed structure, such as the one shown in Figure 3a, where the spots travelled horizontally at constant speed in a wavelike motion, others seemed random and unpredictable. In particular, Figures 2b and 2c showed chaotic behaviour. New stripes formed at apparently random times in apparently random spots. These stripes then moved longitudinally, merging with another stripe. This result is of great interest as it seems to contradict the steady states found by Murray et.al. [8], where the time independent steady state equations were considered.

6 Conclusion and future work

All in all, most of the snake pigmentation patterns observed by Murray were reproduced, with the exception of the longitudinal stripes, which proved computationally intractable and might require an independent model as seen in [4].

However, it is interesting to highlight that unlike Murray's patterns, some unsteady, time dependent patterns were observed. Furthermore they showed chaotic temporal behaviour, even after long times, which in turn means the model is only valid for short times, as most snakes don't change skin patterns after birth, even when shedding [4].

In the future it would be interesting to model a snake's geometry more faithfully, as described in section 4.1, accounting for curvature and three dimensional effects. In Figure 4 we see two examples where this might be important. In figure 4a the stripes in *Bungarus fasciatus*, a species of krait with a very pronounced triangular cross section[3]. In Figure 4b we see a yellow-bellied sea snake with a paddle like tail[4]. Here, the tail is flat to improve the snake's swimming capabilities. The fact that the pattern showcased in the main body of the snake (a longitudinal yellow line) breaks completely as soon as the body becomes paddle like is of great interest. This example would benefit from simulation with a full three dimensional domain.

(a) *Bungarus fasciatus*. Note the heavily keeled, "triangular" cross section

(b) *Pelamis Platurus*. A species of sea snake. Note how the regular pattern breaks in the paddle like flat tail

Figure 4: Banded krait (triangular cross section) and a sea snake (complex tail geometry). The irregular tail shape (very flat, like a paddle or fin) perturbs the main body pattern.

Finally, studying post embryonic pattern development could be potentially interesting. Some snakes, such as the King Cobra (*Ophiophagus hannah*) are born with stripes that are gradually lost until they are almost monochromatic as adults, and not much is known about how and why this happens. In this case the role of diet and food intake might be important, as well as other environmental factors such as their habitat or body temperature. The loss of stripes in adulthood is also seen in other reptiles, most notably the American alligator.

[3]Picture from `https://thailandsnakes.com/venomous/banded-krait-venomous-deadly/`
[4]Picture from: `https://portphillipmarinelife.net.au/species/8107`

References

[1] Turing, A. . (1990) The chemical basis of morphogenesis. *Bulletin of mathematical biology.* [Online] 52 (1), 153–197.

[2] Bourgine, P. & LESNE, A. (2011) *Morphogenesis Origins of Patterns and Shapes. 1st ed. 2011.* [Online]. Berlin, Heidelberg: Springer Berlin Heidelberg.

[3] Hoyle, R. (2006) *Pattern Formation: an Introduction to Methods.* Cambridge: Cambridge University Press.

[4] Murakami, A. et al. (2018) Developmental mechanisms of longitudinal stripes in the Japanese four-lined snake. *Journal of morphology (1931).* [Online] 279 (1), 27–36.

[5] Kowalska, M. & Rupik, W. (2019) Development of endocrine pancreatic islets in embryos of the grass snake Natrix natrix (Lepidosauria, Serpentes). *Journal of morphology (1931).* [Online] 280 (1), 103–118.

[6] Murray, J. . & Myerscough, M. . (1991) Pigmentation pattern formation on snakes. *Journal of theoretical biology.* [Online] 149 (3), 339–360.

[7] Murray, J. D. (2003) *Mathematical biology II: spatial models and biomedical applications.* 3rd ed. New York, N.Y: Springer.

[8] Maini, P. K. et al. (1991) Bifurcating spatially heterogeneous solutions in a chemotaxis model for biological pattern generation. *Bulletin of mathematical biology.* [Online] 53 (5), 701–719.

[9] Hillen, T. & Painter, K. J. (2008) A user's guide to PDE models for chemotaxis. *Journal of mathematical biology.* [Online] 58 (1-2), 183–217.

[10] Burns, K. J. et al. (2020) Dedalus: A flexible framework for numerical simulations with spectral methods. *Physical review research.* [Online] 2 (2), .

[11] Lima, N. et al. (2022) A Time-Splitting Tau Method for PDE's: A Contribution for the Spectral Tau Toolbox Library. *Mathematics in computer science.* [Online] 16 (1), .

7 Appendix

7.1 Numerical procedures and results

In an attempt to reproduce the results presented by Murray et. al. [8], a slightly different numerical procedure was developed. Instead of solving the steady state time independent equations and following the bifurcating branch, the time dependent equations were solved for specific values of the parameters which Murray marks as interesting in [6]. Two different numerical schemes were used, described in the next section

7.1.1 Finite Differences & Stiff solver

As a first attempt a methods of lines discretization of the PDEs was developed. The standard 3 point stencil was used for the Laplacian, and the cell chemotaxis term was discretized in the following way:

$$\partial_x(n\partial_x(v)) \approx \frac{1}{\Delta x^2}\left[n_{i+1/2}(v_{i+1}-v_i) - n_{i-1/2}(v_i - v_{i-1})\right] \quad n_{i+\frac{1}{2}} \approx \frac{1}{2}(n_{i+1}+n_i)$$

Once the system was discretized the equations were coded into MATLAB functions, which were then solved with ode15s, a specialized stiff integrator, and the solution was double checked with ode45.

7.1.2 Spectral solver & Dedalus

As the simple finite differences schemes was not satisfactory a spectral implementation using Dedalus, developed by K. Burns et. al. [10]. In this scheme, periodic boundary conditions were implemented along the horizontal axis of the snake, and Neumann on the longitudinal axis of the snake. This is faithful to the snakes cylindrical coordinates. For this spectral implementation the tau method [11] was used to enforce Neumann boundary conditions.

7.2 Linearization

3 We look in detail at the linearization procedure outlined in section We linearize around the homogeneous steady state found in the previous section

$$n = N + \epsilon u \quad \text{and} \quad c = \frac{N}{1+N} + \epsilon v$$

Then we substitute

$$\epsilon \partial_t u = \epsilon D \nabla^2 u - \alpha \nabla \cdot (N + \epsilon u) \nabla (\frac{N}{N+1} + \epsilon v))) + sr(N + \epsilon u)(-\epsilon u)$$

$$\epsilon \partial_t v = \epsilon \nabla^2 v + s \left(\frac{N + \epsilon u}{N + 1 + \epsilon u} - \frac{N}{1+N} - \epsilon v \right)$$

We can expand the algebraic term as a power series in ϵ to get

$$\frac{N + \epsilon u}{N + 1 + \epsilon u} = 1 - \frac{1}{N + 1 + \epsilon u} = 1 - \frac{1}{N+1} \frac{1}{1 + \epsilon u/(N+1)} = 1 - \frac{1}{N+1} \sum_{i=0}^{\infty} \left(-\frac{\epsilon u}{N+1} \right)^i$$

So

$$\left(\frac{N + \epsilon u}{2N + \epsilon u} - \frac{N}{1+N} - \epsilon v \right) = -\epsilon v + \sum_{i+1}^{\infty} \frac{(\epsilon u)^i}{(N+1)^{i+1}}$$

So dropping terms of order $\mathcal{O}(\epsilon^2)$ or higher and diving through by ϵ we get the linearized equations:

$$\partial_t u = D \nabla^2 u - \alpha N \nabla^2 v - srNu$$

$$\partial_t v = \nabla^2 v + s \left(\frac{u}{(1+N)^2} - v \right)$$

And we still have Neumann Boundary conditions on the border. We can find the dispersion relation by trying the following Ansatz

$$\begin{pmatrix} u \\ v \end{pmatrix} = \begin{pmatrix} \xi \\ \eta \end{pmatrix} e^{i\mathbf{k}\cdot\mathbf{x} + \sigma t}$$

Upon substitution we find that

$$\sigma \begin{pmatrix} \xi \\ \eta \end{pmatrix} = \begin{pmatrix} -(Dk^2 + srN)\xi - k^2 \alpha N \eta \\ -s\xi/(N+1)^2 - (k^2 + s)\eta \end{pmatrix} = \begin{pmatrix} -(Dk^2 + srN) & -k^2 \alpha N \\ -s/(N+1)^2 & -(k^2+s) \end{pmatrix} \begin{pmatrix} \xi \\ \eta \end{pmatrix}$$

We can find σ the characteristic polynomial of the matrix

From the matrix we can also extract relevant information, as the fastest growing mode, using

$$\sigma_{max} = \frac{\partial_k \det(M)}{\partial_k \mathrm{Tr}(M)} = \frac{-2DN^2k^2 - DN^2 s - 4DNk^2 - 2DNs - 2Dk^2 - Ds - N^2 rs - 2Nrs + \alpha rs^2 - rs}{(D+1)(N^2 + 2N + 1)}$$

We are interested in seeing if $\Im(\sigma) \neq 0$ and the node is unstable to see if there might be a pattern. If the node is stable then the snake will be monochromatic ("boring") in terms of its skin patterns.